Available online at www.sciencedirect.com
SCIENCE DIRECT®
Polymer 45 (2004) 1027–1032
polymer
www.elsevier.com/locate/polymer

Crystallization of polycarbonate induced by spinodal decomposition in polymer blends

Manabu Tsuburaya, Hiromu Saito*

Department of Organic and Polymer Materials Chemistry, Tokyo University of Agriculture and Technology, 2-24-16 Nakacho, Koganei-shi, Tokyo 184-8588, Japan

Received 23 May 2003; received in revised form 15 August 2003; accepted 18 November 2003

Abstract

We found that amorphous polycarbonate (PC) can be crystallized in several minutes by blending poly(ethylene oxide) (PEO). When the blends were annealed in the two-phase region below the upper critical solution temperature, highly interconnected two-phase structure characteristic of the spinodal decomposition was developed and then the crystallization occurred in the PC-rich phase during the spinodal decomposition. As the molecular weight of PEO decreased, the crystallization rate decreased and the crystallizable temperature became narrower in spite of the acceleration of the polymeric segmental motion. These results suggest that the crystallization of the PC is not induced by the acceleration of the polymeric segmental motion, but by the up-hill diffusion of the liquid–liquid phase separation via spinodal decomposition. Owing to the competitive progress of the crystallization and the spinodal decomposition, the melting peak of the PC crystallites shifted to lower temperature with increasing annealing temperature.

Keywords: Polycarbonate; Blend; Crystallization

1. Introduction

It is well known that bisphenol-A polycarbonate (PC) is ductile amorphous polymer. Long annealing of the amorphous PC above the glass transition temperature (T_g) can induce the crystallization; i.e. it takes above 6 days for crystallization to start and above 12 days to complete [1,2]. The crystallization of the PC is accelerated by adding plasticizers [3], nucleation agents [4], organic solvents [5–7] and supercritical carbon dioxide [8,9], for instance. The accelerated crystallization is ascribed to the increase of the rate of polymeric segmental motion due to the reduction of the T_g by the plasticization effect [8]. However, it takes at least 1 h to complete the crystallization of the PC.

Recently, we found that PC can be crystallized in several minutes by blending poly(ethylene oxide) (PEO) [10]. In general, the crystallization rate of a crystalline polymer is always delayed by blending it with dissimilar polymers due to the exclusion of the amorphous polymer from a crystal growth front and the interaction between component polymers [11], as demonstrated in poly(vinylidene fluoride) (PVDF)/poly(methyl methacrylate) (PMMA) [12,13], PVDF/poly(ethyl acrylate) [14], poly(ε-caprolactone)/poly(vinyl chloride) [15] and PEO/PMMA [16] systems. Hence, the accelerated crystallization in the PC/PEO blends is rare case in the crystallization of polymer blends.

In this paper, to understand the origin of the crystallization induced by blending, we investigate the crystallization kinetics of the PC/PEO blends with different molecular weights of PEO by polarized optical microscopy and time-resolved Hv light scattering method using a highly sensitive charge-coupled device (CCD) camera system. The crystallization induced by blending is discussed in terms of the competitive progress of liquid–liquid phase separation and crystallization by the results of microscopic observation and differential scanning calorimetry (DSC).

2. Experimental

The polymer specimens used in this study are commercial polymers. PC was supplied by Teijin Chemicals, Ltd; $M_w = 1.47 \times 10^4$. High molecular weight PEO (HM-PEO;

* Corresponding author. Tel./fax: +81-42-388-7294.
E-mail address: hsaitou@cc.tuat.ac.jp (H. Saito).

0032-3861/$ - see front matter © 2003 Elsevier Ltd. All rights reserved.
doi:10.1016/j.polymer.2003.11.026

$M_n = 2.0 \times 10^4$) was supplied by Wako Pure Chemical Industry Co., Ltd and low molecular weight PEO (LM-PEO; $Mn = 2000$) was by Kokusan Chemical Co., Ltd.

The PC and PEO were dissolved at 10 wt% of total polymer in dimethyl formamide. The solution was cast on a cover glass. The solvent was evaporated under a reduced atmosphere of 10^{-2} mmHg at room temperature to prepare a film of 30 μm thick. The cast film was further dried under vacuum (10^{-4} mmHg) for 3 days and then at 120 °C for 24 h to completely remove residual solvent.

The film specimen on a cover glass was melted at $T_a =$ 260 °C for 3 min in a hot stage. Then the melt specimen was rapidly transferred to another hot stage and annealed at desired temperature (T_c). Structural development during the isothermal annealing was observed under an unpolarized optical microscope and also a polarized optical microscope with a sensitive tint plate (Olympus, BX-50). The image data was stored in a personal computer.

The real-time analysis on the isothermal crystallization was also carried out by the light scattering apparatus. The film specimen on a cover glass was melted at $T_a = 260$ °C for 3 min in a hot stage. Then the film specimen was rapidly transferred to another hot stage set on the light scattering stage and annealed at T_c. A polarized He–Ne laser of 632.8 nm wavelength was applied vertically to the film specimen. The scattered light was passed through an analyzer and then onto a highly sensitive CCD camera with 512×512 pixels in a sensor of dimensions 13.3×8.8 mm (Princeton Instruments, Inc., TE/CDD-512-TKM-1). We employed H_v geometry in which the optical axis of the analyzer was set perpendicularly to that of the polarizer. This realizes the time-resolved measurement of a two-dimensional angular distribution of scattered light with 512×512 data points in a time scale of 5 s and that of a one-dimensional one with 512 data points in a time scale of 0.2 s. The input data from CCD camera was digitized by the ST-13X controller. The digitized data were stored in a personal computer for further analysis [17].

The morphology of the annealed specimens was observed under a Hitachi S2100A SEM (scanning electron microscope). For SEM observation, the specimen was rinsed with H_2O (good solvent for PEO) for 10 h at 40 °C. DSC thermogram was recorded by a Rigaku 8230 DSC at a heating rate of 10 °C min^{-1}.

3. Results and discussions

Fig. 1 shows a polarized micrograph of the 70/30 PC/HM-PEO blend observed at annealing temperature of $T_c =$ 180 °C after the temperature drop from $T_a = 260$ °C. Small spherulites with optical anisotropy having a radius of several micrometers are seen. Since the annealing temperature is above the melting temperature of PEO (ca. 60 °C), the existing of the spherulites suggests the crystallization of PC in the blend.

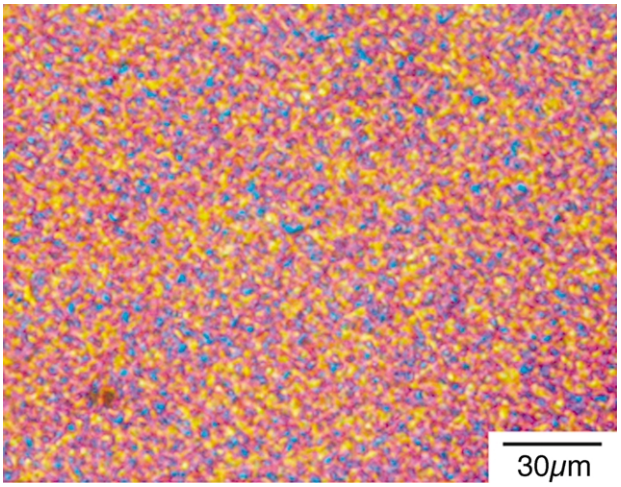

Fig. 1. Polarized micrograph of the 70/30 PC/HM-PEO blend observed at 180 °C after annealing of 30 min.

Fig. 2 shows the DSC thermogram for the spherulites of the PC/HM-PEO blend indicated in Fig. 1. The DSC thermogram of a neat PC is also shown in Fig. 2 for comparison. The neat PC shows a glass transition at around 145 °C. On the other hand, the spherulite of the blend shows an endothermic peak at around 240 °C, while the glass transition of the PC was not detected. Thus the endothermic peak is ascribed to the melting of the PC crystallites and the disappearance of the glass transition is to the reduction of amorphous region in the PC by the crystallization of the PC. These results support the crystallization of the PC in the blend.

To discuss the kinetic aspect of the crystallization of the PC, it is convenient to employ the integrated scattering intensity in Hv mode, i.e. the invariant Q_{Hv} defined by Refs.

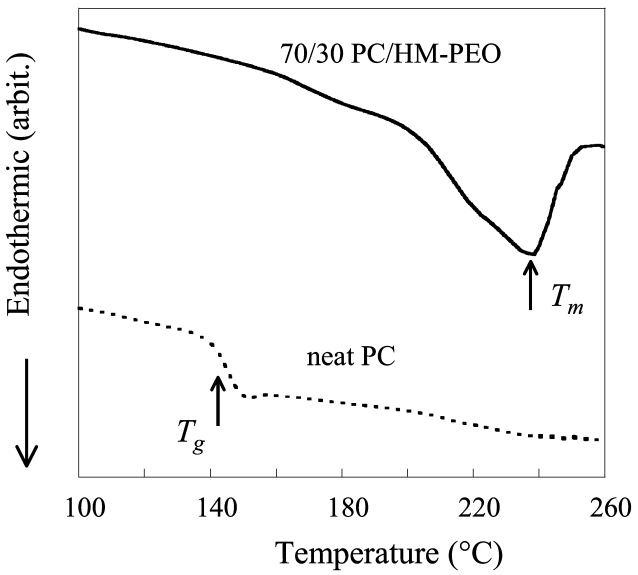

Fig. 2. DSC thermograms of the 70/30 PC/HM-PEO blend and neat PC annealed at 180 °C for 1 h.

[17,18]

$$Q_{Hv} = \int_0^\infty I(q)q^2 \, dq \quad (1)$$

where I is the intensity of scattered light at the scattering vector q, $q = (4\pi/\lambda)\sin(\theta/2)$, λ and θ being the wavelength of the light and the scattering angle, respectively.

The Hv light scattering pattern from the crystallized specimen was a four-leaf clover type. It suggests the scattering from spherulites. In this case, the Q_{Hv} is described by the mean square optical anisotropy $\langle\delta\rangle^2$

$$Q_{Hv} \propto \langle\delta\rangle^2 = \phi_s(\alpha_r - \alpha_t)^2 \quad (2)$$

where ϕ_s is the volume fraction of spherulites and α_r and α_t are the radial and tangential polarizabilities of the spherulite, respectively. Hence, the Q_{Hv} is expected to increase with increasing volume fraction of spherulites and then level off when the spherulites are volume-filled [17,20].

Fig. 3 shows the time variations of invariant Q_{Hv} in the 70/30 PC/PEO blends at various T_c. The Q_{Hv} increases with time and then levels off, as expected from Eq. (2), i.e. ϕ_s increases and attains a maximum when spherulites fill the whole space. The crystallization of the PC was completed at 200 s in the 70/30 PC/HM-PEO blend at $T_c = 180$ °C ($T_c - T_g = 75$ °C : Fig. 3a) and was completed at 500 s in the blend at $T_c = 140$ °C ($T_c - T_g = 35$ °C : Fig. 3b), while the crystallization of neat PC was not completed in spite of the annealing for 2 weeks at $T_c = 180$ °C ($T_c - T_g = 35$ °C : Fig. 4). These results indicate that the crystallization of the PC is exceedingly accelerated by blending PEO. This is contrast to the delay of the crystallization in polymer blends as typically observed in PVDF/PMMA [12,13], PVDF/poly(ethyl acrylate) [14], poly(ε-caprolactone)/poly(vinyl chloride) [15] and PEO/PMMA [16] blends. The accelerated crystallization in the PC/PEO blends is not ascribed to the increase of the mobility by the increase of the $T_c - T_g$.

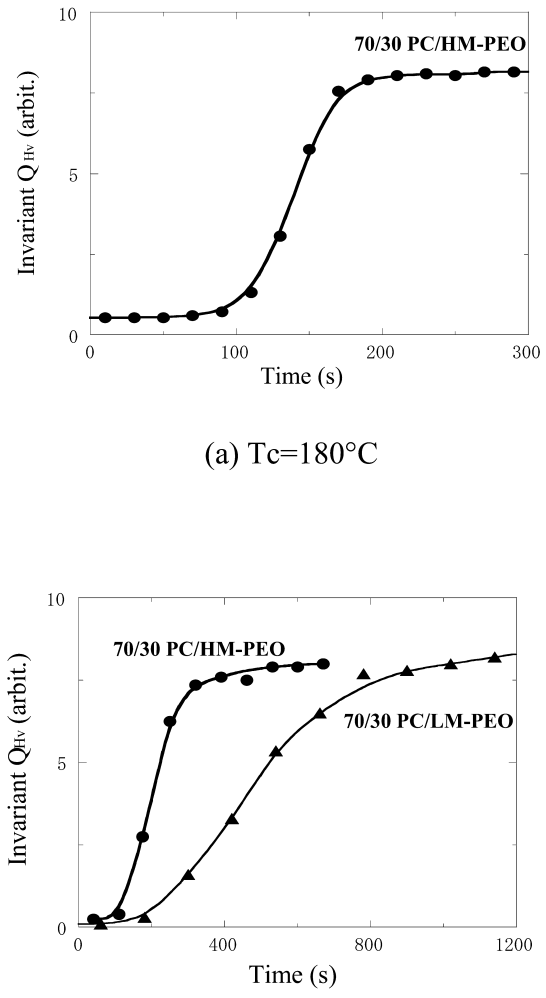

Fig. 3. Time variation of invariants Q_{Hv} in the 70/30 PC/PEO blends annealed at various temperatures.

The interesting result in Fig. 3 is that the crystallization rate of the PC/LM-PEO blend is slower than that of the PC/HM-PEO blend (Fig. 3b). That is, the crystallization rate decreases with decreasing the molecular weight of PEO in spite of the acceleration of the rate of the polymeric segmental motion. This suggests that the crystallization of the PC in the blends is not induced by the increase of mobility by blending PEO.

Fig. 5 shows a structural development of the 70/30 PC/HM-PEO blend after the temperature drop from $T_a = 260$ °C to $T_c = 180$ °C. Initially, no structure was seen. After 65 s, a highly interconnected two-phase structure with unique periodicity was detected under unpolarized microscope, while no structure was detected under polarized microscope (Fig. 5a). The contrast of the two-phase structure became higher with annealing time, as demonstrated by a series of unpolarized micrographs in Fig. 5. The change of the structure is characteristic of the liquid–liquid phase separation via spinodal decomposition. After 100 s, one phase in the two-phase structure began to brighten

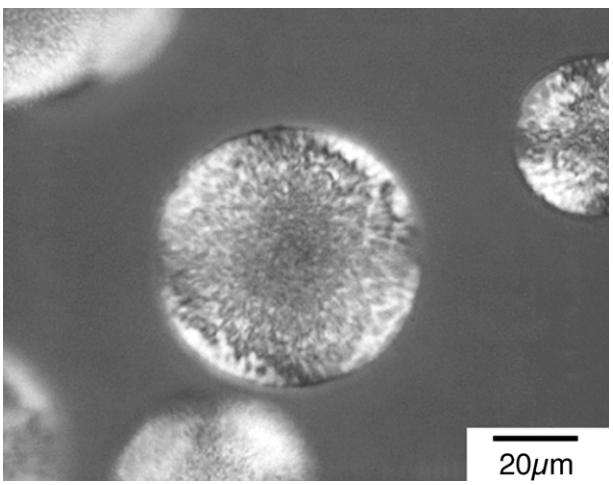

Fig. 4. Polarized micrograph of neat PC annealed at 180 °C for 2 weeks.

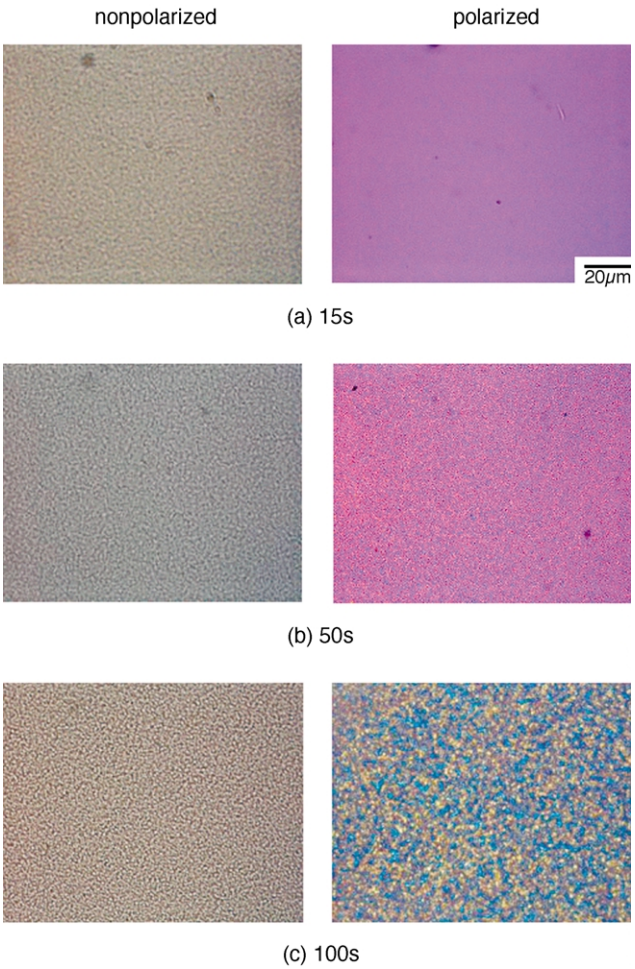

Fig. 5. Microscopic observation of the structural development in the 70/30 PC/HM-PEO blend during isothermal annealing at 180 °C. Left, unpolarized; right, polarized.

under polarized microscope (Fig. 5b), indicating the formation of small spherulites in the PC rich phase. Thus the crystallization occurs during the development of the spinodal decomposition; i.e. the spinodal decomposition precedes and the crystallization of the PC follows.

The development of the interconnected two-phase morphology was also observed in the PC/PEO blends with different compositions, different molecular weights of PEO and also at other annealing temperatures. This type of the behavior is indicated by crosses in Fig. 6. On the other hand, some films of the PC/PEO blends were transparent and no indication of liquid–liquid phase separation could be seen under unpolarized optical microscope. This behavior is indicated by open circles in Fig. 6. On the basis of these observations, the PC/HM-PEO blends were found to exhibit upper critical solution temperature (UCST) behavior (Fig. 6a). The UCST phase boundary shifts to lower temperature and the two-phase region becomes narrower with decreasing the molecular weight of PEO. As shown in Fig. 6b, the PC/LM-PEO blend exhibits an immiscibility loop in the phase diagram. It consists of UCST and low critical solution

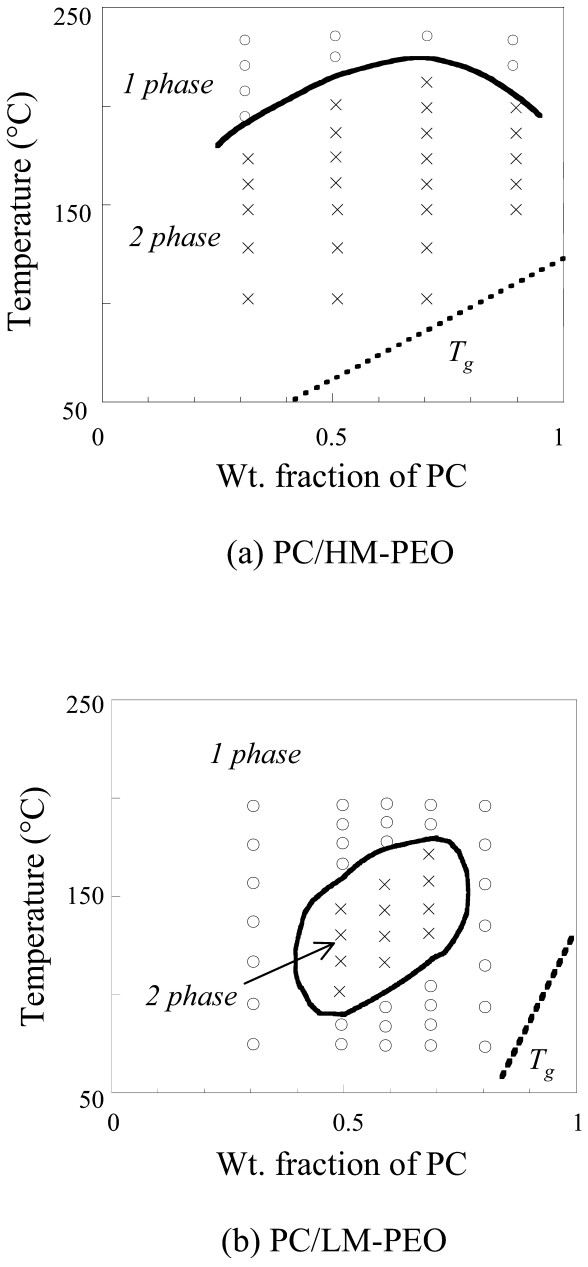

Fig. 6. Phase diagram of the PC/PEO blends: (○) transparent, (×) opaque.

temperature (LCST) phase boundaries, as demonstrated in poly(ethylene glycol)/water [19], polypropylene (PP)/hydrogenated oligo(cyclopetadiene) [20] and PP/hydrogenated oligo(stylene-co-indene) blends [21].

The crystallization of the PC occurs at $T_c = 100–210$ °C in 70/30 PC/HM-PEO blend while it occurs at $T_c = 140–170$ °C in 70/30 PC/LM-PEO blend. That is, the crystallization of the PC occurs in the temperature region in which liquid–liquid phase separation via spinodal decomposition takes place (crosses in Fig. 6). On the other hand, the crystallization of the PC does not occur in the temperature region in which liquid–liquid phase separation does not take place (open circles in Fig. 6). This is why the Q_{Hv} of the 70/30 PC/LM-PEO blend is

lacked in Fig. 3a; i.e. the crystallization occurs at $T_c = 180$ °C in the PC/HM-PEO blend while it does not occur in the PC/LM-PEO blend. Thus, the crystallizable temperature becomes narrower with decreasing the molecular weight of PEO in spite of the acceleration of the polymeric segmental motion. These results suggest that the crystallization of the PC is not induced by the increase of the mobility, but by the up-hill diffusion of the liquid–liquid phase separation via spinodal decomposition [22].

The crystallization of the PC does not occur in PC/PMMA blends in which two-phase structure exists but the concentration fluctuation does not grow by the temperature drop or annealing. This suggests that the crystallization of the PC is not induced by the existence of the concentration fluctuation, but by the up-hill diffusion. The crystallization of the PC/PEO blend induced by the up-hill diffusion via spinodal decomposition is schematically shown in Fig. 7. It is well known that the spinodal decomposition renders the periodic concentration fluctuation. The growth of the concentration fluctuation is realized by the 'up-hill diffusion'; i.e. molecules diffuse into A-rich region from B-rich region. So, in the PC/PEO blend, PC chains are forced to move from the PEO-rich region to the PC-rich region (Fig. 7a) and then the nucleation of PC crystallites is induced (Fig. 7b), while PEO chains are forced to move from the PC-rich region to the PEO-rich region. That is, the crystallization of PC with the growth of concentration fluctuation associated with demixing of PC

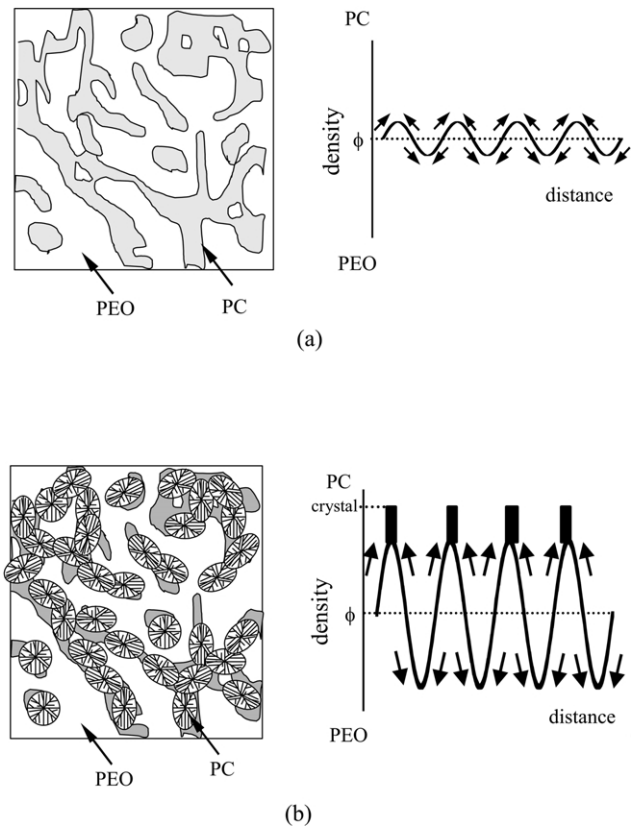

Fig. 7. Schematics of crystallization process in the PC/PEO blends.

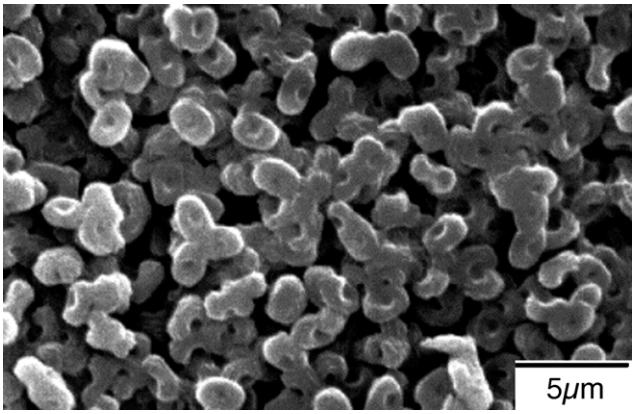

Fig. 8. Scanning electron micrograph of the 70/30 PC/HM-PEO blend annealed at 200 °C for 1800 s.

and PEO. This means the competitive progress of the spinodal decomposition and the crystallization; i.e. the crystallizable chains are supplied to the embryo of the crystallites under the thermodynamic driving force for the liquid–liquid phase separation. Hence, the crystallization could be accelerated by the induction of each crystallite due to the progress of the spinodal decomposition.

Fig. 8 shows a SEM micrograph for the structure of the 70/30 PC/HM-PEO blend demonstrated by polarized and unpolarized micrographs in Figs. 1 and 5. The PEO-rich phase having a size of a few micrometers could be rinsed with water. This may support the existing of the two-phase structure in the blends. The remaining materials seen in the micrograph are the PC spherulites. The shape of the PC spherulites is ellipsoidal. The PC spherulites are not isolated, but are connected. Such ellipsoidal and connected spherulites may be ascribed to the liquid–liquid phase separation via spinodal decomposition that occurs competitively with the crystallization. In other words, the PC spherulites grow in the elongated and connected PC-rich phase obtained by the spinodal decomposition. Owing to the

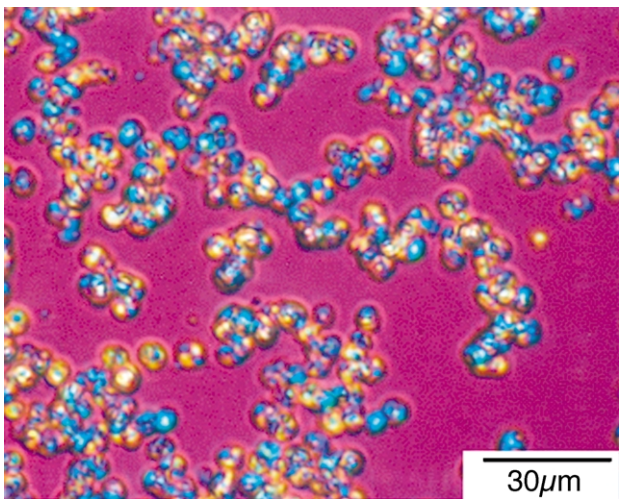

Fig. 9. Polarized micrograph of the 30/70 PC/HM-PEO blend observed at 160 °C after annealing of 3600 s.

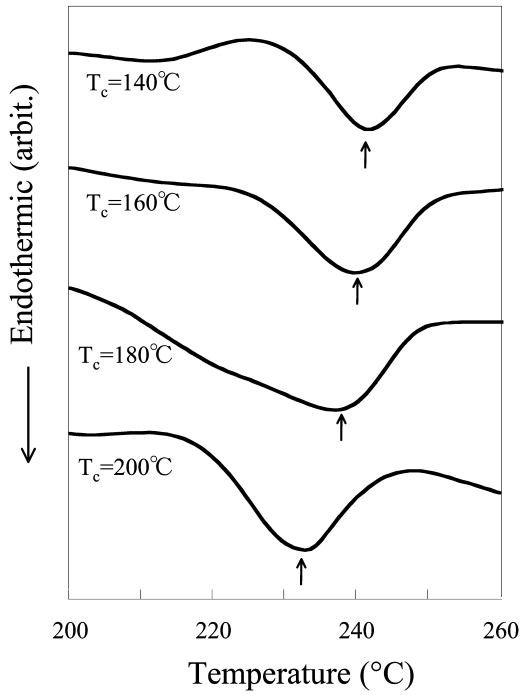

Fig. 10. DSC thermograms of the 70/30 PC/HM-PEO blends obtained at various annealing temperatures for 1 h.

competitive progress of the spinodal decomposition and the crystallization, large connected spherulites having a size of several ten micrometers were also obtained at PC poor composition (30/70 PC/HM-PEO blends), as shown in Fig. 9.

Fig. 10 shows the DSC thermograms of the 70/30 PC/HM-PEO blends obtained at various annealing temperatures. The melting peak of the PC crystallites shifts to lower temperature with increasing annealing temperature T_c. This result is opposite to melting behavior expected by the Hoffmann–Weeks theory [23,24] in which melting peak shifts to higher temperature with increasing the T_c associating with the increase of the lamellar thickness. As discussed in Fig. 6, the PC/PEO blends exhibit the UCST type phase behavior. As the quench depth from the UCST phase boundary decreases (T_c increases), the concentration fluctuation by the spinodal decomposition becomes smaller and the volume fraction of the crystalline polymer decreases. According to the Flory–Huggins theory, the melting temperature decreases with decreasing the volume fraction of the crystalline polymer due to the depression effect of the melting temperature [25]. This may interpret the decrease of the melting temperature of the PC with increasing the T_c. Thus the characteristic melting behavior of the PC/PEO blends shown in Fig. 10 may be ascribed to the competitive progress of the crystallization and the liquid–liquid phase separation.

4. Conclusion

We found that amorphous PC can be crystallized in several minutes by blending PEO. The crystallization of the PC may be induced by the up-hill diffusion of the liquid–liquid phase separation via spinodal decomposition. Owing to the competitive progress of the liquid–liquid phase separation and the crystallization, connected spherulites were obtained and the melting temperature decreased with increasing crystallization temperature. The detail of the competitive progress will be discussed by the quantitative analysis of the time resolved Hv and Vv light scattering methods.

References

[1] Kampf G. Kolloid-Z 1960;50:1972.
[2] Turska E, Przygocki W, Maslowski M. J Polym Sci, Part C 1968;16:3373.
[3] Gallez F, Legras R, Mercier JP. J Polym Sci, Polym Phys 1976;14:1367.
[4] Bailly CH, Daumerie M, Legras R, Mercier JP. J Polym Sci, Polym Phys 1985;23:751.
[5] Sheldon RP, Blakey PR. Nature 1962;14:172.
[6] Turska E, Janeczek H. Polymer 1979;20:855.
[7] Mercier JP, Groeninckx G, Lesne M. J Polym Sci, Part C 1967;16:2059.
[8] Chiou JS, Barlow JW, Paul DR. J Appl Polym Sci 1985;30:3911.
[9] Beckman E, Porter RS. J Polym Sci, Polym Phys 1987;25:1511.
[10] Tsuburaya M, Saito H. Fiber Prepr Jpn 2001;56:62.
[11] Stein RS. Pure Appl Chem 1991;63:941.
[12] Wang TT, Nishi T. Macromolecules 1977;10:421.
[13] Saito H, Okada T, Hamane T, Inoue T. Macromelocules 1991;24:4446.
[14] Briber RM, Khoury F. Polymer 1987;28:38.
[15] Ong CJ, Price FP. J Polym Sci, Polym Symp 1978;63:59.
[16] Martuscelli E, Pracella M, Wang PY. Polymer 1984;25:1097.
[17] Lee CH, Saito H, Inoue T. Macromolecules 1993;26:6566.
[18] Koberstein J, Russell TP, Stein RS. J Polym Sci, Polym Phys 1979;17:1719.
[19] Saeki S, Kuwahara N, Nakata M, Kaneko M. Polymer 1976;17:685.
[20] Cimmino S, DiPace E, Karasz FE, Martuscelli E, Silvestre C. Polymer 1993;34:972.
[21] Lee CH, Saito H, Goizueta G, Inoue T. Macromolecules 1996;29:4274.
[22] Matsuura M, Saito H, Nakata S, Imai Y, Inoue T. Polymer 1992;33:3210.
[23] Lauritzen Jr JI, Hoffman JD. J Res Natl Bur Stand 1960;64A:73.
[24] Hoffman JD, Weeks JJ. J Res Natl Bur Stand 1962;66A:13.
[25] Nishi T, Wang TT. Macromolecules 1975;8:909.